VOL. 11, NO. 8, APRIL 2016 ISSN 1819-6608
ARPN Journal of Engineering and Applied Sciences

www.arpnjournals.com

EXPERIMENTAL STUDY ON BOTTOM BOUNDARY LAYER BENEATH SOLITARY WAVE

Bambang Winarta[1], Nadiatul Adilah Ahmad Abdul Ghani[1], Hitoshi Tanaka[2], Hiroto Yamaji[2] and Mohammad Fadhli Ahmad[3]
[1]Faculty of Civil Engineering & Earth Resources, Universiti Malaysia Pahang, Gambang, Pahang, Malaysia
[2]Department of Civil Engineering, Tohoku University, Sendai, Japan
[3]School of Ocean Engineering, Universiti Malaysia Trengganu, Kuala Terengganu, Terengganu, Malaysia
E-Mail: fadhli@umt.edu.my

ABSTRACT

A tsunami as long wave and an oscillatory wave moves into shoaling water have behavior similar to solitary wave and therefore comprehension on its bottom boundary layer characteristics come to be essential key on near-shore sediment transport modeling. In the present study, the hydraulics phenomena of solitary wave are studied in deep through experiments utilizing a closed conduit generation system. This result was examined by analytical and numerical laminar solution. Moreover, wave friction factor is discussed based on the present laboratory experiment and previous studies of (Sumer *et al*., 2010); (Vittory and Blondeaux, 2011, 2012). As conclusions, in-consistent critical Reynolds number was found for solitary wave case. This observable fact is distinct difference with sinusoidal wave case which has consistency in critical Reynolds number. As a main conclusion that a new generation system proposed in the present study will be able and applicable to shore up an experiment on sediment transport induced by solitary wave.

Keywords: solitary wave, boundary layer, closed conduit generation system.

INTRODUCTION

Comprehension on sea bottom boundary layer characteristics is primacy in near-shore sediment transport modeling. A tsunamis or seismic sea wave has behavior resembling to solitary waves. Besides that, as an oscillatory wave moves into shoaling water, its amplitude becomes progressively higher, the crests become shorter and the trough becomes longer and flatter and it is similar to solitary wave. Because of these reasons, laboratory experiment and numerical experiment studies concerning solitary wave boundary layer will be necessary to hold up in its application for practical purposes such as sediment transport.

Solitary wave boundary layer characteristics on laminar flow have been studied in both laboratory experiments and also in theoretical study. Wave flume with free surface was commonly used on previous studies. One of them is (Liu *et al*., 2007); their experimental system is assisted by Particle Image Velocimetri (PIV) to measure velocity in the thin boundary layer. It is concluded that the experiments fall in laminar regime and still cannot investigate in transitional and turbulent regimes. Indeed, wave flume experiment facilities have difficulty to attain high Shield's number. Another problem is hard to reproduce near-bed characteristics at practical scale. Due to these inconveniences, a proper generation set up to shore up an experiment on sediment transport induced by solitary wave is highly required.

To figure out some difficulties found in the previous sediment transport experiment, closed conduit and oscillating water tunnel are used. The purpose is to reproduce near-bed hydrodynamic and sediment transport phenomena at a realistic scale. Recently, (Sumer *et al*., 2010), carried out laboratory experiment using an oscillating water tunnel on investigation turbulent solitary wave boundary layer. However, it will be practically difficult to generate boundary layer flow exactly corresponds to solitary wave motion because of restorative force in a tunnel, which may induce oscillating motion with flow reversal. Beside that U-shape oscillating water tunnel has difficulty to do periodical measurement. As we know that one wave cycle is not sufficient to make an adequate amount of sediment movement and consequently, it will be less of accuracy.

In the present study, the hydraulics phenomena of solitary wave are studied in deep through experiments utilizing a closed conduit generation system. Furthermore by combining with previous experiments of (Sumer *et al*., 2010) and numerical approach by (Vittori and Blondeaux, 2011, 2012) diagram for wave friction factor is obtained.

EXPERIMENTAL CONDITION

The detail explanation of a new laboratory generation system such as: general sketch, generation system mechanism was given in the previous publication (Tanaka *et al*., 2011). A series of experiments with different value of Reynolds number has been carried out using a closed conduit generation system.

Laser Dopller Velocimeter (LDV) installed in generation set-up measured instantaneous velocity at 17-20 points in the vertical direction at 10 ms intervals, the sample of instantaneous horizontal velocity at three different elevation can be seen in Figure-1. The mean velocity was obtained by averaging over 50 wave cycles, while the α values were found out by fitting equation (1) to the measured free stream velocity. Experimental Reynolds number (R_e) written in Table-1 were estimated by following equation.

$$R_e = \frac{U_c^2}{\upsilon\alpha} \quad (1)$$

U_c	=	the maximum velocity under wave crest,
υ	=	kinematic viscosity,
α	=	α value was determined by fitting the exact solution of solitary wave to the measured free stream velocity.

The various conditions in present experiment are summarized in Table-1. Parameter T(s) in the second column of this table is period of rotating disc.

Table-1. Experimental conditions.

	T (s)	υ (cm^2/s)	U_c (cm/s)	α (s^{-1})	R_e
Case 1	16.90	0.0116	78.7	0.95	5.64 x 10^5
Case 2	15.36	0.0116	78.5	0.88	6.06 x 10^5
Case 3	16.99	0.0114	81.3	0.81	7.34 x 10^5

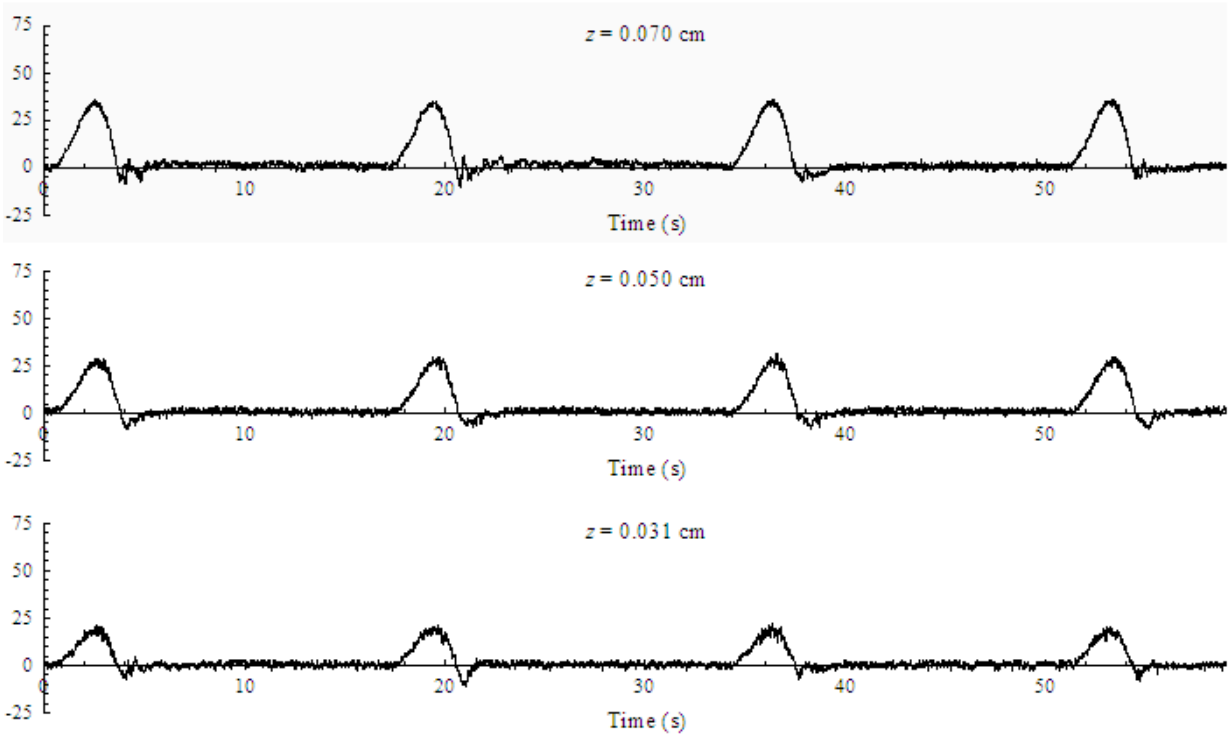

Figure-1. Instantaneous horizontal velocity (Case 1, R_e = 5.64 x 10^5) in 3 different measured elevations.

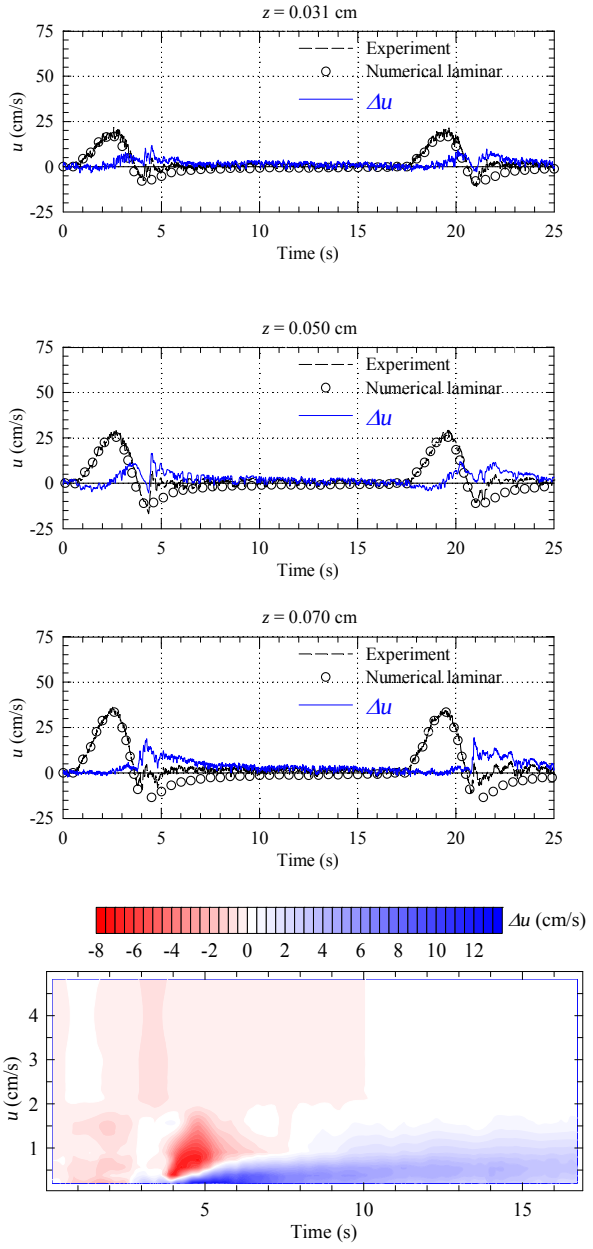

Figure-2. Quantitative value of Δu ($\Delta u = u_{experiment} - u_{lam.}$).

Parameter Δu is used to know the quantitative difference value between velocity obtained from the present laboratory experiment and numerical laminar computation and defined as subtraction of numerical laminar computation from the measured stream wise velocity ($\Delta u = u_{experiment} - u_{lam.}$). The calculation results of Δu is performed in Figure-2. It can be clearly observed that velocity during accelerating phases is recover to laminar, Δu value is in between -3 cm/s to 3 cm/s and during decelerating phases Δu value is getting higher, it is in -10 cm/s to 18 cm/s for Case 1, R_e = 5.64 x 10^5. This is clearly indicating reduction process of flow reversal in the near bottom due to turbulence generation.

RESULTS AND DISCUSSIONS

Shear stress estimation

Bed shear stress quantity controls the sediment transport process. In oceans the total bed shear stress is summation of bed shear stress caused by tidal currents as unidirectional flows and also oscillatory wave. It is general known that grain of sediment will start motion when critical bed shear stress is exceeded. Therefore correct calculation of bottom shear stress is prior step needed in sediment transport calculation and analysis.

Local bottom shear stress can be estimated from linear fitting measured velocity in the near bottom or in the viscous layer (δ_v). It can be expressed as:

$$\frac{u}{u*} = \frac{u* z}{\upsilon} \quad (2)$$

$$\delta_v = \frac{11.6\upsilon}{u*} \quad (3)$$

u	=	the vertical velocity in the boundary layer,
$u*$	=	the shear velocity,
z	=	the vertical coordinate.

And bottom shear stress (τ_0) is expressed by following equation,

$$\frac{\tau_0}{\rho} = u*|u*| \quad (4)$$

ρ = the fluids density.

The other formulation to calculate bottom shear stress (τ_0) is using Manning equation. This expression is frequently used to asses this quantity.

$$\frac{\tau_0}{\rho} = \frac{g n^2}{R_h^{1/3}} \overline{U}\left|\overline{U}\right| \quad (5)$$

g	=	acceleration gravity,
n	=	Manning roughness coefficient,
R_h	=	(R_h = A/P, where A is wetted area and P is wetted perimeter),
U	=	depth averaged velocity.

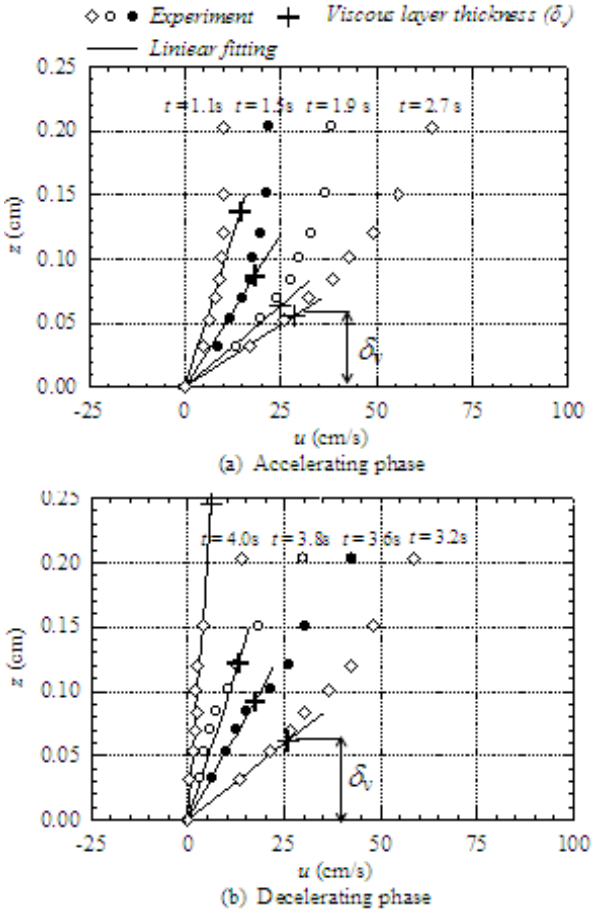

Figure-3. Estimation of shear velocity.

Shear velocity is calculated by doing linear fitting to measured velocity and cross-checking the suitable viscous layer thickness simultaneously. Figure-3 illustrate the viscous layer thickness in variation of time, it is getting lower during accelerating phase up to wave crest and then gradually higher during decelerating phase. Bottom shear stress is square of shear velocity as shown in equation (4). In the present study this quantity is also estimated by Manning equation. Manning roughness coefficient (n) used in bottom shear stress calculation is 0.01 (for glass), this (n) value reflect closed conduit material of generation system applied in the present experiment.

(Keulegan, 1948) have derived the expressions inside boundary layer for velocity and bottom shear stress in the spatial variation, considering linearized boundary layer equation in the laminar flow regime. And then, it is converted by (Tanaka *et al*., 1998) for both expressions in temporal variation and written as follows:

$$\frac{u}{U_c} = sec\,h^2(\alpha t) - \frac{2}{\sqrt{\pi}} \int_0^{\infty} sec\,h^2 \left\{ \alpha t - \left(\frac{\beta' z}{\phi} \right)^2 \right\} e^{-\phi^2} d\phi \quad (6)$$

$$\frac{\tau_0}{\rho U_c^2} \frac{\sqrt{R_e}\sqrt{\pi}}{4} = \frac{4U_c^2}{\sqrt{R_e}\sqrt{}} \int_0^{\infty} \sec h^2\left(\alpha t + \phi^2\right) \tan h\left(\alpha t + \phi^2\right) d\phi \quad (7)$$

in which;

$$\beta' = \frac{1}{2}\sqrt{\frac{\alpha}{\upsilon}} \quad (8)$$

Figure-3 illustrated the bottom shear in a variation of Reynolds number with different methods of calculation. During accelerating phase bottom shear stress has close agreement with analytical laminar solution, it means during this phase velocity distribution in viscous layer is in laminar distribution. At R_e = 5.64 x 10^5, during accelerating phase up to end of decelerating phase, bottom shear stress has a good agreement with analytical laminar solution, it has meaning velocity distribution is almost laminar. However, slight deviation from analytical laminar solution occurs after end of deceleration period, it is indicating that velocity distribution near wall has already moved to higher flow regime. Other characteristics indicate flow regime changing is appearing spike in instantaneous horizontal velocity. Detail analysis of horizontal and vertical velocity distribution can be seen in the previous publication (Tanaka *et al*., 2011). When R_e = 6.06 x 10^5 deviation from analytical laminar solution come earlier than previous case and bottom shear stress during flow reversal is almost zero. Quite different behavior when R_e = 7.34 x 10^5, deviation from analytical laminar solution is getting higher and come earlier than 2 previous cases.

From Figure-3 we also can observe the magnitude of bottom shear stress using Manning equation is giving 3 times different with 2 other methods. The Manning equation estimates the bottom shear stress as a function of square of velocity per depth as shown in equation (5). In case of unsteady flow condition, this relation is not always correct and as consequence bottom shear stress is also not accurate.

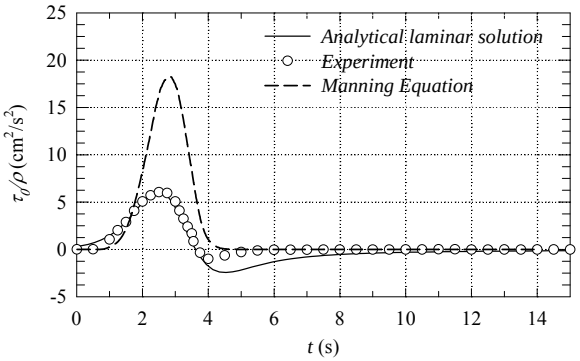

(a) Case 1, R_e = 5.64 x 10^5

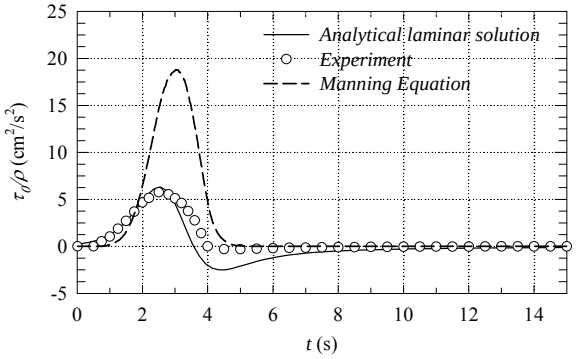

(b) Case 2, R_e = 6.06 x 10^5

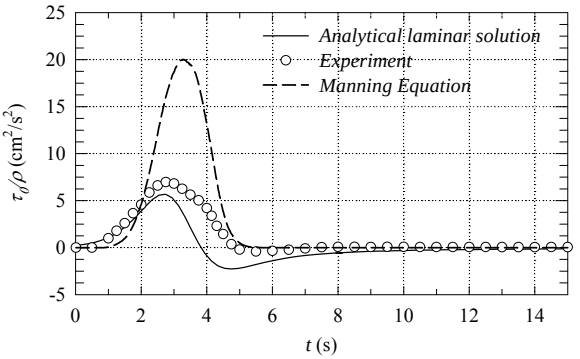

(c) Case 3, R_e = 7.34 x 10^5

Figure-4. Bottom shear stress.

Wave friction factor

Wave friction factor (f_w) is dimensionless parameter used to estimate bed shear stress induced by wave. This parameter is related to the Shields parameter β for unidirectional current. The wave friction factor can be computed by following equation from measured bottom shear stress,

$$f_w = \frac{2\tau_{0max}}{\rho U_c^2} \quad (9)$$

$\tau_{0\,max}$ = the maximum bottom shear stress.

Analytical laminar solution for wave friction factor under solitary wave can be obtained from the equation (7) and then expressed in term of Reynolds number as following equation,

$$f_w = \frac{1.71}{\sqrt{R_e}} \quad (10)$$

The wave friction factor from the previous experiment study and direct numerical simulation (DNS) are plotted in similar Figure with present laboratory experiment as shown in Figure-5 and among them show a good agreement with equation (10), although R_e attain at R_e = 2.7 x 10^6, it has to be 5 times of R_e = 5 x 10^5 as critical Reynolds number. The cases of present experiments with R_e = 5.64 x 10^5, R_e = 6.06 x 10^5 and R_e = 7.34 x 10^5 are above of critical Reynolds number but the wave friction factors fall in analytical laminar solution (equation (10)). It is caused by transition to turbulence phenomenon happened in decelerating period, while during accelerating phase flows recover to laminar where the maximum bottom shear stress occurred. As a conclusion, wave friction factor under solitary wave also show in-consistency of critical Reynolds number, it is similar to boundary layer thickness.

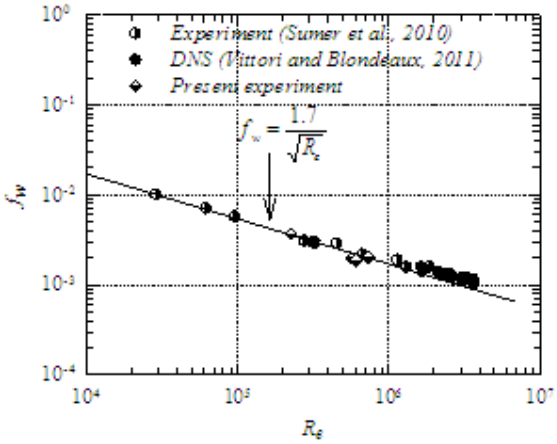

Figure-5. Wave friction factor.

Sinusoidal wave versus solitary wave

Figures-6 and 7 are summary three criteria: wave friction factor, phase difference and boundary layer thickness in two different of wave cases: sinusoidal wave and solitary wave. Sinusoidal wave case has consistency in critical Reynolds number in terms of boundary layer thickness, phase difference and wave friction factor as display in Figure-6 (Jensen *et al.,* 1989; Tanaka and Thu, 1994). A dissimilar observable fact can be found in solitary wave case which has inconsistency of critical Reynolds number. A critical Reynolds number proposed by (Sumer *et al*., 2010) is at 5 x 10^5 and this value is similar to DNS simulation result by (Vittori and Blondeaux, 2011). The same finding also was found from the present laboratory experiments of Case 1 with Reynolds number (R_e) = 5.64 x 10^5, this case confirmed a good agreement with previous findings in a stability diagram. After comprehensive investigation of the present experiments data, an inconsistency of critical Reynolds number is also found in wave friction factor and boundary layer thickness as shown in Figure-7.

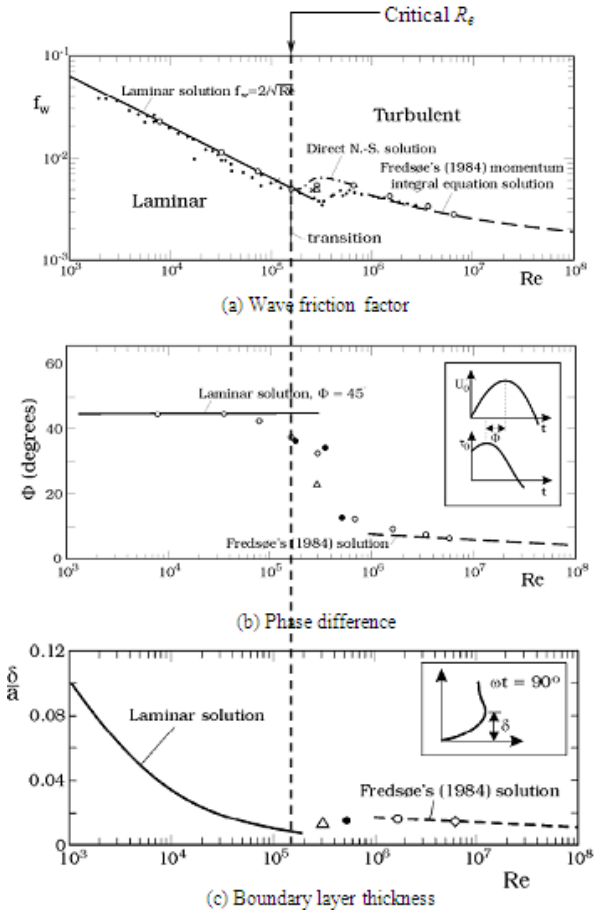

Figure-6. Characteristics of sinusoidal wave.

CONCLUSIONS

A series of experiments with different value of Reynolds number has been carried out using a closed conduit generation system. Estimation and evaluation of some parameters have been done: shear stress and wave friction factor. A new knowledge can be found from this present study is in-consistency of critical Reynolds number in terms of boundary layer thickness and wave friction factor for solitary wave. This observable fact is distinct difference with sinusoidal wave case which has consistency in critical Reynolds number of boundary layer thickness, phase difference and wave friction factor.

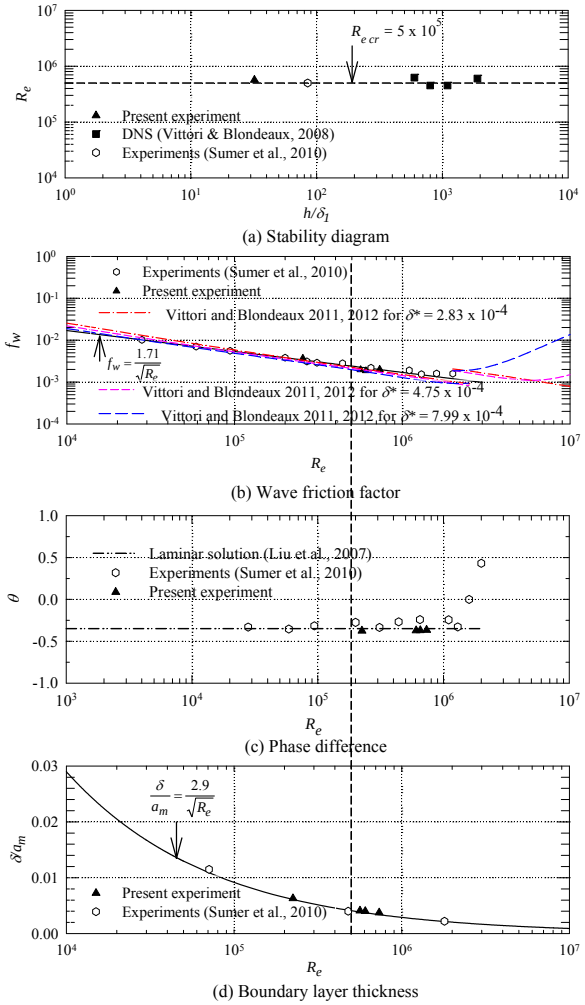

Figure-7. Characteristics of solitary wave.

REFERENCES

Blondeaux, P. and Vittori, G. 2012. RANS modeling of the turbulent boundary layer under solitary wave. Coastal Eng., 60, pp. 1-10

Fredsøe, J. 1984. Turbulent boundary layer in wave-current motion. Journal of Hydraulics Engineering, ASCE, 110(HY8), pp. 1103-1120.

Jensen, B., Sumer, B.M. and Fredsøe, J. 1989. Turbulent oscillatory boundary layer at high Reynolds number. J. Fluid Mech., 206, pp. 265-297.

Keulegan, G. H. 1948. Gradual damping of solitary waves. U.S. Department of Commerce, National Bureau of Standards. RP1895, 40, pp. 487-498.

Liu, P. L. -F., Park, Y. S. and Cowen, E. A. 2007. Boundary layer flow and bed shear stress under a solitary wave. J. Fluid Mech., 574, pp. 449-463.

Sleath, J.F.A. 1987. Turbulent oscillatory flow over rough beds. J. Fluid Mech., 182, pp. 369-409.

Sumer, B. M., Jensen, P. M., Sørensen, L. B., Fredsøe, J., Liu, P. L.-F and Cartesen, S. 2010. Coherent structures in wave boundary layers. Part 2. Solitary motion. J. Fluid Mech., 646, pp. 207-231.

Suntoyo and Tanaka, H. 2009. Numerical modeling of boundary layer flows for a solitary wave. J. Hydro-Environ. Res., 3(3), pp. 129-137.

Tanaka, H., Bambang Winarta, Suntoyo and Yamaji, H. 2011. Validation of a new generation system for bottom boundary layer beneath solitary wave, Coastal Eng., 59, pp. 46-56

Tanaka, H., Sumer, B. M. and Lodahl, C. 1998. Theoretical and experimental investigation on laminar boundary layers under cnoidal wave motion. Coastal Eng. J. 40(1), pp. 81-98

Tanaka, H. and Thu, A. 1994. Full-range equation of friction coefficient and phase difference in a wave-current boundary layer. Coastal Eng., 22, pp. 237-254.

Vittori, G. and Blondeaux, P. 2011. Characteristics of the boundary layer at the bottom of a solitary wave. Coastal Eng. 58, pp. 206-213.